Theoretical & Applied Mechanics Letters 9 (2019) 229-235

Contents lists available at ScienceDirect

Theoretical & Applied Mechanics Letters

journal homepage: www.elsevier.com/locate/taml

Letter

Pendulum systems for harvesting vibration energy from railroad tracks and sleepers during the passage of a high-speed train: A feasibility evaluation

Franco E. Dotti[a,*], Mauricio D. Sosa[b]

[a] *Grupo de Investigación en Multifísica Aplicada, Universidad Tecnológica Nacional, Facultad Regional Bahía Blanca. Consejo Nacional de Investigaciones Científicas y Técnicas. Argentina*
[b] *Grupo de Investigación en Multifísica Aplicada, Universidad Tecnológica Nacional, Facultad Regional Bahía Blanca. Argentina*

HIGHLIGHTS

- We aim to recover energy from vibrations during the passage of a high-speed train.
- A harvester based on the rotatory dynamics of the parametric pendulum is considered.
- A sustained rotation is strictly required to generate a usable amount of power.
- Rotations are not hard to obtain, but depend on the choice of initial conditions.
- With a suitable design, a single harvester could generate an average power of 5–6 W.

ARTICLE INFO

Article history:
Received 25 March 2019
Received in revised form 23 April 2019
Accepted 5 May 2019
Available online 10 May 2019
This article belongs to the Dynamics and Control.

Keywords:
Energy harvesting
Parametric pendulum
Railroad safety
Train induced vibration

ABSTRACT

We evaluate the feasibility of recovering energy from the vibrations of track and sleepers, during passage of a high-speed train, by means of a pendulum harvester. A simple mathematical model of the parametric pendulum is employed to obtain numerical predictions, while measured data of vibration tests during the passage of a Thalys high-speed train are considered as input forcing. Since a sustained rotation is the most energetic motion of a pendulum, the possibility of achieving such state is evaluated, taking into account the influence of initial conditions, damping and other factors. Numerical simulations show that rotating pendulum harvesters with sufficiently low viscous damping could be able to generate a usable average power on the order of 5–6 W per unit. Considering a modular arrangement of devices, such energy is enough to feed variety of rail-side equipment, as wireless sensors or warning light systems. However, a suitable choice of initial conditions could be a difficult task, leading to the need of a control action.

Unprotected railroad crossings and derailments due to mechanical failures represent the two most significant sources of railroad accidents all over the world [1, 2]. In order to improve safety, warning light systems and structural health monitoring (SHM) sensors are strictly necessary. But in remote areas, the lack of electrical infrastructure represents a major impediment for the installation of rail-side equipment.

A potential solution to this problem is given by the use of autonomous systems, powered by energy harvested from vibrations of the track and/or sleepers caused by passing trains. The vibration of the track constitutes a time-limited excitation, since the motion is only significant for a short period of time. For high speed trains (HST), a typical duration of track vibration is on the order of 3–5 s [3, 4]. Despite their short duration, these vibrations can be highly energetic. Thus, several technologies have been developed and tested aiming to scavenge that energy, being the most common devices piezoelectric [5, 6], electromagnetic [7] and mechanical [8–11]. An interesting comparison among several devices can be found in Ref. [1]. Piezoelectric and inductive voice coil devices were reported to generate an average power on the order of 4–12 mW [5], which is enough to ener-

* Corresponding author.
E-mail address: fdotti@frbb.utn.edu.ar (F. E. Dotti).

http://dx.doi.org/10.1016/j.taml.2019.03.005

gize SHM sensors. To feed systems with higher power demands, as warning lights at grade crossings, an average power on the order of 10 W is required [1]. Mechanical devices have been considered in such situation, being rack and pinion [9], hydraulic [10] and cam-based [11] the most employed devices.

The vertical parametric pendulum was firstly proposed as an energy harvester by Prof. Marian Wiercigroch, aiming to extract energy from the ocean waves [12–15]. The idea is simple and intuitive: a pendulum vertically excited by an external motion at a given (averaged) frequency is able to achieve a rotational motion. Thus, a generator coupled to the pendulum axis could extract a part of that kinetic energy and produce electrical energy. In this article, we address the possibility of recovering energy during the passage of an HST by means of the same concept: a pendulum harvester attached to rails or sleepers. A simple mathematical model is employed to perform numerical simulations and evaluate the applicability of the concept. To ensure the existence of rotations, the physical dimensions of the harvester are defined in terms of the predominant excitation frequency in vertical direction, which is the fundamental bogie passage frequency [16]. The influence of initial conditions is evaluated, in order to avoid coexisting non rotating states as oscillating motion or chaos [14]. To count with realistic results, the input excitations correspond to experimental data measured during the passage of a Thalys HST [3].

A schematic diagram of a pendulum harvester is shown in Fig. 1. The pendulum consists of a bob of mass m and a rod of length l. The axis of the pendulum is mounted on a rigid frame, which is in turn fixed to a rigid base. The base is subjected to an external motion $Y = Y(t)$, provided by the vibration of the track or sleeper. Besides, a generator coupled to the pendulum axis is able to extract a constant torque J from the pendulum motion. By means of Lagrange's equation for single degree-of-freedom non-conservative systems, the governing equation of such system can be expressed as

$$ml^2\ddot{\theta} + b\,l^2\dot{\theta} + ml\left(\ddot{Y} + g\right)\sin\theta + \kappa J\,\mathrm{sgn}\,\dot{\theta} = 0, \tag{1}$$

where $\theta(t)$ is the angle measured from the downward hanging position (positive in counter-clockwise direction), l is the length of the rod, m is the mass of the pendulum bob, g is gravity and b is the viscous damping coefficient. Assuming that excitation takes place from $t = 0$ on, κ triggers energy extraction at a time $t_0 > 0$ in the following form: if $t < t_0$, then $\kappa = 0$; if $t \geq t_0$, then $\kappa = 1$. Thus, the instantaneous power extracted from the system is given by

$$P = \kappa J\left|\dot{\theta}\right|, \tag{2}$$

while the average power can be expressed as

$$\overline{P} = \frac{1}{t_s - t_0}\left(\int_{t_0}^{t_s} J\left|\dot{\theta}\right|\,\mathrm{d}t - E_0\right), \tag{3}$$

where t_s the time required by the pendulum to stop completely at its rest position and E_0 is the initial energy of the system, given by

$$E_0 = \frac{1}{2}ml^2\dot{\theta}_0^2 + mgl\left(1 - \cos\theta_0\right) - \frac{1}{2}b\,l^2\dot{\theta}_0^2. \tag{4}$$

The magnitude E_0 can be assumed as the energy required to restore initial conditions θ_0 and $\dot{\theta}_0$ after energy extraction, by means of the servomotor and the gear-belt system of Fig. 1. Thus, E_0 is subtracted from the generation in Eq. (3).

To obtain realistic simulations, the input excitation of Eq. (1) corresponds to time histories of acceleration measured during the passage of a Thalys HST. The measurements were performed during homologation tests of the HST track between Brussels and Paris, and gently provided by Degrande and Schillemans [3], who made the data available to other researchers.

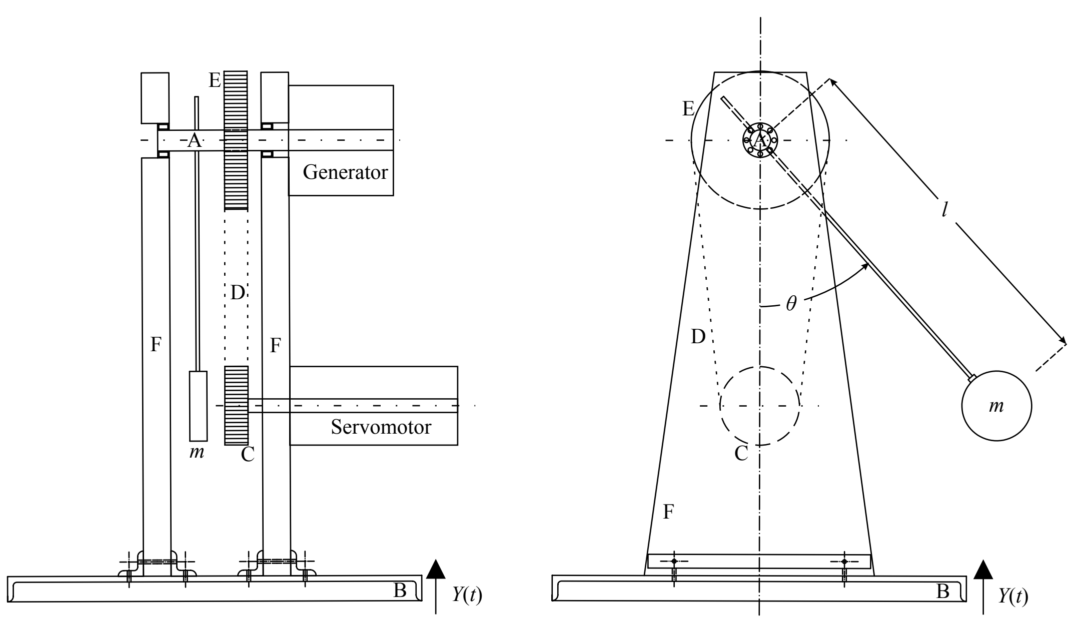

Fig. 1. Schematic diagram of a pendulum harvester (side views). A: pendulum axis, B: pendulum base, attached to the track or sleeper, C-D-E: gear-belt coupling between the pendulum axis and the servomotor, which provides the initial conditions to the pendulum, F: frame.

Four different data sets are considered in our work, at different train speeds v: t_{12}, t_{22}, and t_{23}, corresponding to measurements on the rail, and t_{21}, measured on the sleeper. These vibrational data is presented in Fig. 2. The denominations follow the nomenclature of Ref. [3].

Since the parametric pendulum a potential well system, a period-1 rotation represents its most energetic state [15] (from now on, we refer to period-1 rotations simply as rotations). Thus, the determination of the physical magnitudes l and m must be related to the ability of sustaining such rotational state. For a parametric pendulum with a sinusoidal excitation given by $Y(t) = A\cos(\Omega t)$ and m can be estimated by a relatively simple procedure. Setting $\kappa = 1$, Eq. (1) can be written in a dimensionless form as

$$\theta'' + \beta\theta' + [1 + p\cos(\omega\tau)]\sin\theta + \mu\,\mathrm{sgn}\,\dot{\theta} = 0, \tag{5}$$

where p and ω are the dimensionless parameters of amplitude and frequency of excitation, respectively. Besides, β and μ are also dimensionless parameters, related to viscous damping and energy extraction, respectively. Those are given by

$$p = \frac{A\Omega^2}{g}, \quad \omega = \frac{\Omega}{\omega_0}, \quad \beta = \frac{b}{m\omega_0}, \quad \mu = \frac{J}{mgl}, \tag{6}$$

where $\omega_0 = (g/l)^{1/2}$ is the natural frequency of the pendulum. In Eq. (5), $(\cdot)'$ denotes differentiation with respect to dimensionless time $\tau = \omega_0 t$. Essentially, Eq. (5) resembles the classic parametric pendulum [17], considering the influence of dry friction [18].

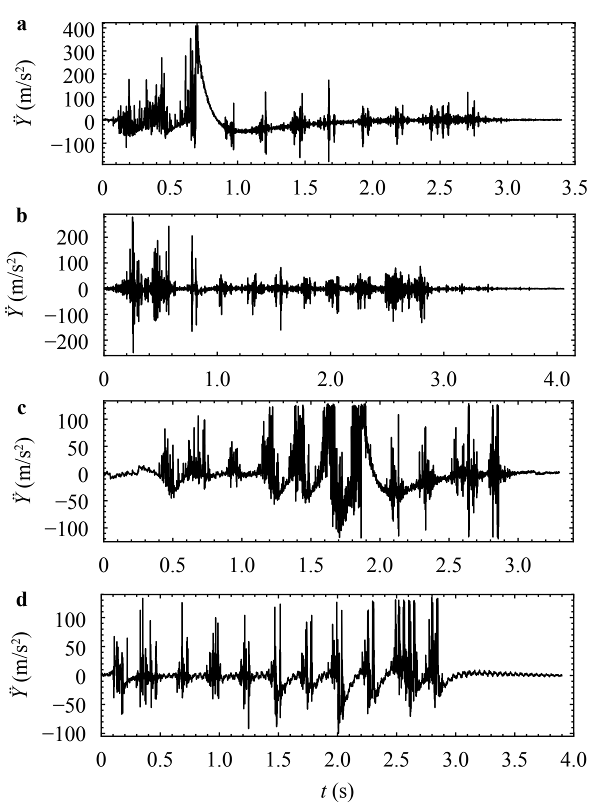

Fig. 2. Time histories of vertical acceleration during the passage of the Thalys HST [3] used in this work. **a** v = 265 km/h (t_{12}), **b** v = 271 km/h (t_{22}), **c** v = 289 km/h (t_{23}), **d** v = 256 km/h (t_{21}).

For $\mu = 0$ in Eq. (5), it can be assumed that rotation is a possible steady state of the system if the analytical conditions of Lenci et al. [19] are fulfilled. Now, in order to consider $\mu \neq 0$, such conditions have been slightly modified after some numerical experiments, to produce

$$p_{\mathrm{SN}} < p < \omega^{3/4} p_{\mathrm{PD}}, \qquad \omega > 1, \tag{7}$$

being

$$p_{\mathrm{SN}} = \frac{2\beta\left(1+\omega^2+\omega^4\right)}{\omega+\omega^3} + \mu\omega^{3/5} \tag{8}$$

and

$$p_{\mathrm{PD}} = p_{\mathrm{SN}}\sqrt{1 + \frac{\left(\beta^{-1} - \pi\omega^{-1}\right)^2}{\left[\omega\int_0^{\pi}\left(f_0(\theta)\right)^{-3}\mathrm{d}\theta \int_0^{\pi} f_0(\theta)\,\mathrm{d}\theta\right]^2}}, \tag{9}$$

where $f_0(\theta)$ is the solution for the unperturbed pendulum. The fulfilling of Eq. (7) implies that the pair (p, ω) lies inside a particular area in the parameter space p–ω called "rotation zone" [17]. This is shown in Fig. 3. Now, given the definition of ω in Eq. (6), we can define

$$l = \frac{g\,\omega^2}{\Omega^2}, \tag{10}$$

where Ω is known and $\omega > 1$, to meet the second condition of Eq. (7). Then, also assuming b as a known magnitude and after calculating p from Eq. (6), m must be chosen appropriately to meet $p_{\mathrm{SN}} < p < \omega^{3/4}\,p_{\mathrm{PD}}$.

For a sinusoidal excitation, the fulfillment of Eq. (7) ensures the existence of rotations. For stochastic excitations (as the vibration of a passing train), an analogy can be drawn to provide a clue to obtain such motion. It is not possible to define values for A and Ω in the case of a stochastic motion. Hence, rotations cannot be ensured for a given combination of parameters. However, a mean amplitude A_S and a predominant excitation frequency Ω_S still can be obtained from the stochastic signal. For a passing train, Ω_S is the fundamental bogie passage frequency [16], namely $\Omega_S = 2\pi v/L_b$, where v is the train speed and L_b is the distance between bogies. Using A_S and Ω_S, suitable magnitudes of m and l can be determined through Eq. (6)-(9).

Numerical simulations are performed, in order to evaluate the rotational behavior of the pendulum during the passage of the Thalys HST. We aim to quantify the power that could be generated and to address the influence of initial conditions and vis-

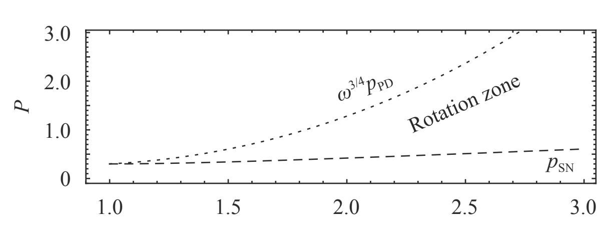

Fig. 3. Rotation zone of the classic parametric pendulum, represented in the parameter space p–ω. β = 0.1, μ = 0.

cous damping. Initially, the importance of achieving a sustained rotational motion is studied, to generate a usable amount of power. In Figs. 4 and 5, two different time responses of the pendulum during the forcing event t_{12} are presented. Identical configuration is employed in both cases, except for the initial condition of angular velocity, set as –2.2 s^{-1} and –8.0 s^{-1}, respectively. In Fig. 4, the parametrically forced pendulum reaches and maintains a counterclockwise rotation, completing a total of 20 revolutions ($\theta = 40\pi$). It stops after t_s = 5.43 s, allowing an average power generation of 4.10 W. This is indicated by the horizontal dotted line in Fig. 4(c). In Fig. 5, the motion of the forced pendulum is rotational at first. But right after starting energy extraction (at t_0 = 0.4 s), the motion becomes oscillatory. At $t_s \approx$ 3.75 s, the pendulum stops at its hanging position. Power generation is much lower in this case: 0.73 W. These results are reasonable in view of the definition of average power, Eq. (3), as the integral of angular velocity over time is greater if rotations are achieved.

Gray lines in Figs. 4 and 5, represent the response of the unforced pendulum (i.e., Y = 0 in Eq. (1)), for the same initial conditions. Comparing with the forced pendulum (black lines), the influence of track vibration in the dynamics can be observed. Clearly, much more vibratory energy is transferred to the pendulum if a sustained rotation is reached.

Figures 4 and 5 also evidence that a suitable choice of initial conditions θ_0 and $\dot{\theta}_0$ is essential to successfully obtain a rotational motion [14]. Thus, a quantification of the amount of power that could be generated for different realistic initial states is required. The influence of initial conditions in nonlinear systems is commonly addressed by constructing the associated basins of attraction, i.e. the sets of initial states leading to a particular attractor. Now, basins are meaningless for a pendulum in the case of time-limited excitations since the responses are entirely transient, being the rest position the only possible attractor. However, a resemblance can be raised: high power generation levels are associated to initial conditions leading to a sustained rotation. As a general rule, it can be established that if $\overline{P}$ > 3 W is generated, it means that rotations are reached and maintained.

Figure 6 shows contour plots of average power, for every initial states fulfilling $-\pi \le \theta_0 \le \pi$ and $-4\omega_0 \le \dot{\theta}_0 \le 4\omega_0$ [15]. Figure 6(a) corresponds to setting ω = 2.5, for a pendulum under the excitation of event t_{12}. The well-known fractal dynamics of the parametric pendulum is observed [13, 14]. This fractalization is due to the dynamics of the parametric pendulum but also to the stochasticity of the excitation [20]. For trajectories starting inside the two symmetrical basins in the neighborhood of $\left(\theta_0,\ \dot{\theta}_0\right) = (\pm\pi/2,\ \mp 18\ \mathrm{s}^{-1})$, numerical simulations indicate a maximum average power of 5.9 W. However, initial conditions must be very precise to obtain such power, being 3–5 W a more realistic prediction.

As could be expected, the fractal topology evolves as ω is var-

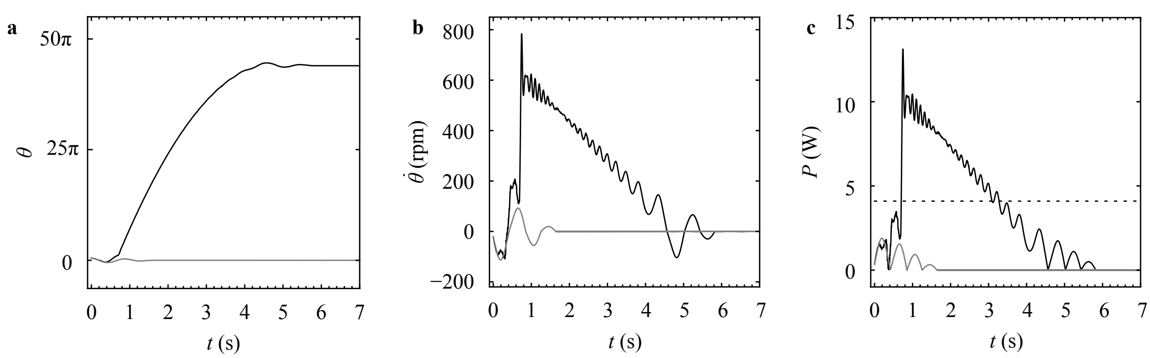

Fig. 4. Time responses of the pendulum. **a** Angular position, **b** angular velocity and **c** generated power. Settings: ω = 3.0, b = 0.0045 kg/s, l = 144.33 mm, m = 0.5 kg, t_0 = 0.4 s and J_0 = 0.16 J. Initial conditions: $\theta_0 = \pi/2$, $\dot{\theta}_0 = -2.2$ s^{-1} (–21.0 rpm). Reference: "–": unforced pendulum with forcing of event t_{12}; "$\cdots$": generated average power with forcing of event t_{12}. Rotations are successfully reached.

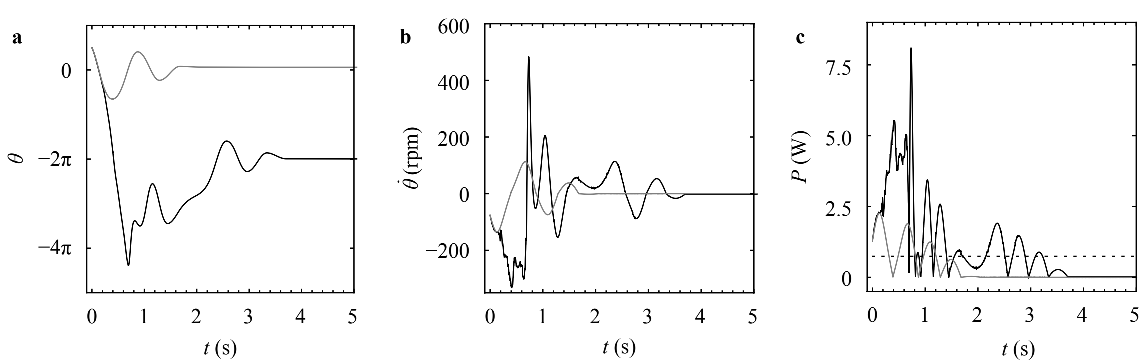

Fig. 5. Time responses of the pendulum. **a** Angular position, **b** angular velocity and **c** generated power. Settings: ω = 3.0, b = 0.0045 kg/s, l = 144.33 mm, m = 0.5 kg, t_0 = 0.4 s and J_0 = 0.16 J. Initial conditions: $\theta_0 = \pi/2$, $\dot{\theta}_0 = -8.0$ s^{-1} (–76.4 rpm). Reference: "–": unforced pendulum with forcing of event t_{12}; "$\cdots$": generated average power with forcing of event t_{12}. Rotations are not successfully reached.

ied. In Fig. 6(b), ω is increased up to 3. The basins observed in the previous example are identifiable and keep their size, but move to zones of higher initial velocity. Realistic power levels of 3–6 W could be obtained, which are higher than those of example in Fig. 6(a). This is logical since rotations become faster as ω increases [17]. Maximum levels of 7.7 W are observed in this case in the neighborhood of $\dot{\theta}_0 = \pm 5\ \mathrm{s}^{-1}$, with $-\pi/4 < \theta_0 < \pi/4$.

Similarly, Fig. 6(c) shows that less power could be generated if ω is decreased to 2. This is because rotations are slower. Besides, reducing ω imply reducing l (note that $l = 64.14$ mm in this example). Thus, the pendulum may result to be very short (in practical terms) to have a massive bob, as we consider in the previous two examples. A reduction of both mass and length implies an increase of β and μ. Such increase moves upwards the curve p_{SN} of Fig. 3, thus placing our system closer to the lower border of the rotation zone [17, 21]. Due to this situation, smaller basins are obtained, and rotations become even more difficult to achieve.

From the three examples above, it follows that ω must be as high as possible. Now, the lower boundary of the rotation zone (Fig. 3) grows exponentially from $\omega = 3$ on (p_{SN} provides a good approximation of such boundary up to $\omega = 3$). In practical terms, rotations of the pendulum are impossible to obtain for $\omega > 4.5$. Thus, a reasonable choice seems to be $\omega = 3$, which is considered in the next examples.

An average power of 3–4 W is expected in the case of event t_{23}, as shown in Fig. 6(d). Topology is very different if compared to Fig. 6(b), confirming that dynamics can be strongly influenced by the vibratory pattern of the track. This represents a drawback, preventing a priori determination of a suitable set of initial conditions which work for all cases. Nevertheless, in view of the high power generation predicted by the simulations, the implementation of a control action of low power consumption could be a viable option [22, 23]. The servomotor schematized in Fig. 1 could be an option to implement such control [23].

Figure 6(e) considers the vibration of a sleeper as input motion (event t_{21}). Simulations indicate that rotations are very difficult to reach, as $\overline{P} > 3$ W is obtained only for a reduced set of initial conditions. Given the low power generation, a control action is not a choice. Thus, energy extraction seems to be not viable in this case. An even worse situation is presented in Fig. 6(f) (event t_{22}), as rotations cannot be obtained. In both examples, the passage of the train produces a low vibration. The average amplitude A_S is small and so is p, from Eq. (6). The system is placed almost over the curve p_{SN} in Fig. 3 and thus obtaining rotations is a very difficult task.

Damping must be as low as possible in order to maximize power generation [24]. For all the examples presented, b = 0.01 kg/s was assumed as a realistic magnitude [8]. But given the influence of damping in the dynamics of the parametric pendulum [18], a situation of increased damping must be considered. In a real life application, such increase can be generated by a problem with the bearings, a progressive misalignment of the pendulum axis, a sudden modification in the orientation of the bob or, in general terms, any malfunction caused by the long term operation condition of the system. In fact, due to malfunctions, damping can become of a very complex nature. We do not intend to analyze in depth the topological changes in the dynamics produced by damping, but only its influence as a mere dissipative energy mechanism. Thus, we simplify the treatment by only increasing the damping coefficient b (or β). A progressive increase in damping is considered in Fig. 7. In Fig. 7(a), β has

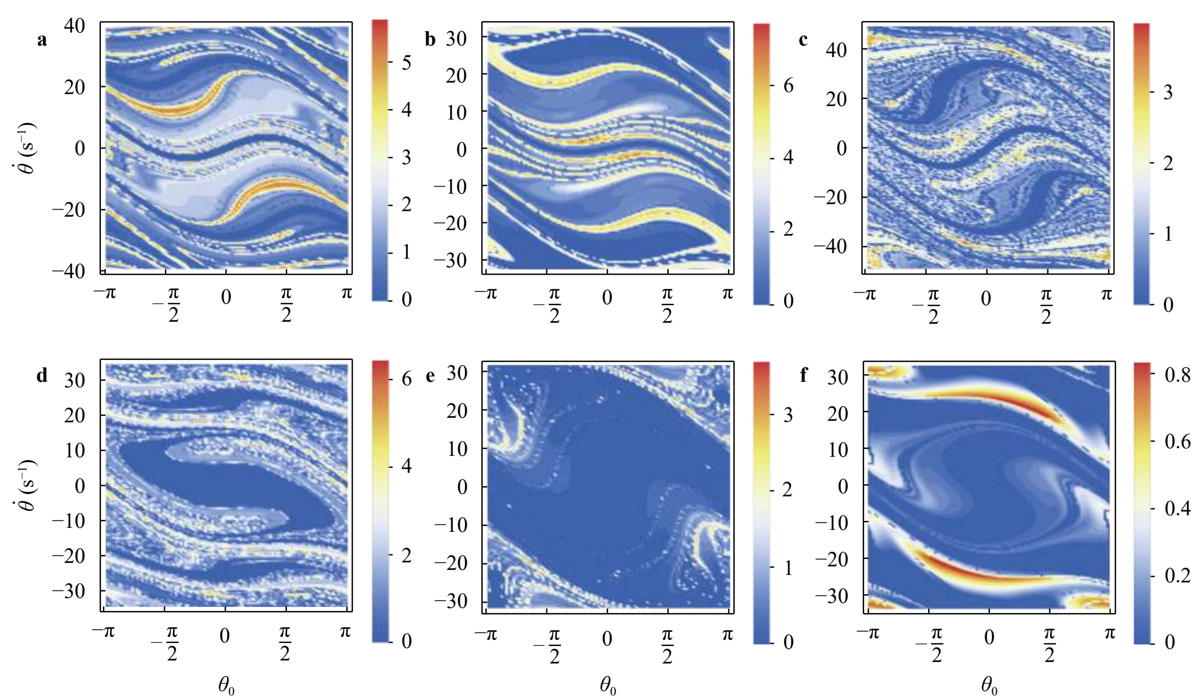

Fig. 6. Output average power levels (in W) as function of initial conditions, corresponding to forcing events of Fig. 2. **a** Event t_{12}, $\omega = 2.5$ (l = 100.23 mm). **b** Event t_{12}, $\omega = 3.0$ (l = 144.32 mm). **c** Event t_{12}, $\omega = 2.0$ (l = 64.14 mm). **d** Event t_{23}, $\omega = 3.0$ (l = 121.35 mm). **e** Event t_{21}, $\omega = 3.0$ (l = 154.65 mm). **f** Event t_{22}, $\omega = 3.0$ (l = 138.01 mm). In all cases: m = 0.5 kg, J_0 = 0.25 J, b = 0.01 kg/s and t_0 = 0.4 s.

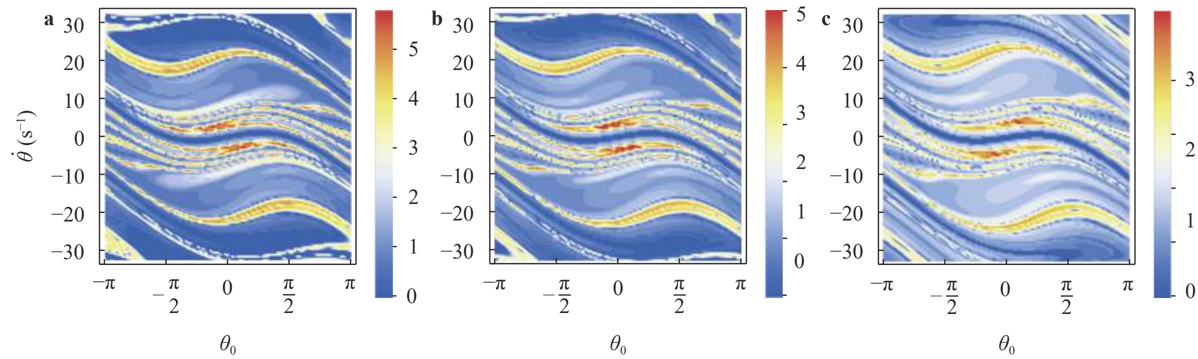

Fig. 7. Output average power levels (in W) as function of initial conditions, considering event t_{12} as input forcing, with ω = 3.0, l = 144.32 mm, m = 0.5 kg, J_0 = 0.25 J and t_0 = 0.4 s. Different amounts of damping considered: **a** b = 0.1 kg/s (β = 0.024), **b** b = 0.23 kg/s (β = 0.055) and **c** b = 0.42 kg/s (β = 0.102).

been raised 10 times with respect to Fig. 6(b) (β = 0.0024). Power generation is lower since rotation basins are small, but still 3–5 W could still be obtained relatively easy. Such tendency continues in Fig. 7(b): 3–4 W of average power are still possible to obtain, but basins are very small. Rotations are very difficult to obtain in the example of Fig. 7(c). Again, the system is placed very close to the curve p_{SN}, and energy extraction could not be possible. However, damping has been raised 40 times with respect to the case of Fig. 6(b), and rotations are still reached.

Finally, some comments on the influence of torque J and triggering time t_0. With a very low damping, the amount of energy that could be extracted from the pendulum motion is almost independent of the torque J. But value of J depends on power requirements. For example, if warning lights at grade crossings must be fed, the energy must be extracted in a few seconds, and thus J must be as high as possible. Since J is proposed to be constant in Eq. (1), energy extraction must start after a time $t_0 > 0$ in order to allow the pendulum to increase its kinetic energy and produce rotations. Energy extraction as proposed in Eq. (1) is a possibility, which is equivalent to consider a bi-linear dry friction. However, different strategies could be considered in order to avoid the delay t_0 and optimize generation. For example, the torque J could be applied gradually, or assumed as proportional to the angular velocity of the pendulum. From a trial and error tactic, we assumed t_0 = 0.4 s and J = 0.25 J in all the examples. This allows in most cases developing rotations (as long as they are feasible) and stopping the pendulum completely after a time t_S, which is approximately equal to the duration of the input acceleration signal.

The possibility of recovering energy from the passage of HST was addressed. Due to the simplicity of its mechanisms, a device based on the parametric pendulum was considered as harvester. After several simulations, we concluded that if viscous damping is sufficiently low (0.01 kg/s), a single pendulum with length 120 mm and mass 0.5 kg could be able to generate average power levels on the order of 5–6 W. This represents an encouraging prediction, since 10 W is the required power to illuminate one high efficiency light-emitting diode (LED) lamp [1].

A sustained rotational motion of the pendulum is strictly required to generate a usable amount of power. This should not represent a problem since rotations are a common response of the parametric pendulum. However, their associated basins (i.e. the sets of initial conditions producing rotations) depend of the input forcing. Now, given the high level of average power predicted by the simulations, the implementation of a control action of low power consumption could be a choice [22, 23] to overcome such drawback.

The behavior of the potential harvester against an increase in damping was addressed. Simulations showed that rotations are robust, as 3–5 W could still be obtained after rising damping 10 times. Nevertheless, energy must be saved due to a latent need for an active control system, which should be fed from the harvester itself. Consequently, keeping a low viscous damping represents a crucial topic.

Acknowledgements

The authors would like to thank the support of Secretary of Science and Technology of UTN, CONICET, the National Agency for Scientific and Technological Promotion and Engineering Department of UNS. Professor Franco Dotti dedicates this article to the beloved memory of his childhood friend Lucía Trotz (1975-2018).

References

[1] A. Pourghodrat, C.A. Nelson, S.E. Hansen, et al., Power harvesting systems design for railroad safety, in: Proc. Inst. Mech. Eng. Part F J. Rail Rapid Transit. 228 (2014) 504–521.

[2] A.W. Evans, Fatal train accidents on Europe's railways: 1980-2009, Accid. Anal. Prev. 43 (2011) 391–401.

[3] G. Degrande, L. Schillemans, Free field vibrations during the passage of a thalys high-speed train at variable speed, J. Sound Vib. 247 (2001) 131–144.

[4] D.P. Connolly, G. Kouroussis, P.K. Woodward, et al., Field testing and analysis of high speed rail vibrations, Soil Dyn. Earthq. Eng. 67 (2014) 102–118.

[5] C.A. Nelson, S.R. Platt, D. Albrecht, et al., Power harvesting for railroad track health monitoring using piezoelectric and inductive devices, in: Proc. SPIE - Int. Soc. Opt. Eng. - Act. Passiv. Smart Struct. Integr. Syst. 69280R (2008) .

[6] J. Li, S. Jang, J. Tang, Implementation of a piezoelectric energy harvester in railway health monitoring, sensors smart struct, Technol. Civil Mech. Aerosp. Syst. 9061 (2014) 90612Q.

[7] J.J. Wang, G.P. Penamalli, L. Zuo, Electromagnetic energy har-

vesting from train induced railway track vibrations, in: Proc. 2012 8th IEEE/ASME Int. Conf. Mechatron. Embed. Syst. Appl. MESA (2012) 29–34.

[8] G. Gatti, M.J. Brennan, M.G. Tehrani, et al., Harvesting energy from the vibration of a passing train using a single-degree-of-freedom oscillator, Mech. Syst. Signal Process. 66–67 (2016) 785–792.

[9] C.A. Nelson, S.R. Platt, S.E. Hansen, et al., Power harvesting for railroad track safety enhancement using vertical track displacement, in: Proc. SPIE. Smart Structures and Materials 7288 (2009) 728811.

[10] C.A. Nelson, A. Pourghodrat, M. Fateh, Energy harvesting from vertical deflection of railroad track using a hydraulic system for improving railroad track safety, Des. Manuf. (2011) 259–266.

[11] A. Pourghodrat, C.A. Nelson, A system for generating electricity using the passage of train wheels for improving railroad track safety, in: 36th Mech. Robot. Conf. 4 (2012) 1025–1031.

[12] X. Xu, E. Pavlovskaia, M. Wiercigroch, et al., Dynamics and control of vertically driven pendulum for energy extraction from sea waves, World Renew. Energy Congr. (2005) 945–950.

[13] X. Xu, M. Wiercigroch, M.P. Cartmell, Rotating orbits of a parametrically-excited pendulum, Chao. Solit. Fract. 23 (2005) 1537–1548.

[14] F.E. Dotti, F. Reguera, S.P. Machado, A review on the nonlinear dynamics of pendulum systems for energy harvesting from ocean waves, in: PANACM 2015 - 1st Pan-American Congr. Comput. Mech. Conjunction with 11th Argentine Congr. Comput. Mech. (2015).

[15] K. Nandakumar, M. Wiercigroch, A. Chatterjee, Optimum energy extraction from rotational motion in a parametrically excited pendulum, Mech. Res. Commun. 43 (2012) 7–14.

[16] S.H. Ju, H.T. Lin, J.Y. Huang, Dominant frequencies of train-induced vibrations, J. Sound Vib. 319 (2009) 247–259.

[17] M.J. Clifford, S.R. Bishop, Rotating periodic orbits of the parametrically excited pendulum, Phys. Lett. A. 201 (1995) 191–196.

[18] F.E. Dotti, F. Reguera, S.P. Machado, Damping in a parametric pendulum with a view on energy harvesting, Mech. Res. Commun. 81 (2017) 11–16.

[19] S. Lenci, E. Pavlovskaia, G. Rega, et al., Rotating solutions and stability of parametric pendulum by perturbation method, J. Sound Vib. 310 (20089) 243–259.

[20] A. Najdecka, S. Narayanan, M. Wiercigroch, Rotary motion of the parametric and planar pendulum under stochastic wave excitation, Int. J. Non. Linear Mech. 71 (2015) 30–38.

[21] R.W. Leven, B. Pompe, C. Wilke, et al., Experiments on periodic and chaotic motions of a parametrically forced pendulum, Phys. D: Nonlinear Phenom. 16 (1985) 371–384.

[22] F. Reguera, F.E. Dotti, S.P. Machado, Rotation control of a parametrically excited pendulum by adjusting its length, Mech. Res. Commun. 72 (2016) 74–80.

[23] A.S. de Paula, M.A. Savi, Controlling chaos in a nonlinear pendulum using an extended time-delayed feedback control method, Chaos, Solitons and Fractals 42 (2009) 2981–2988.

[24] K. Nandakumar, M. Wiercigroch, A. Chatterjee, Optimum energy extraction from rotational motion in a parametrically excited pendulum, Mech. Res. Commun. 43 (2012) 7–14.